

# BER performances of downlink and uplink NOMA in the presence of SIC errors over fading channels

Ferdi Kara<sup>1</sup> , Hakan Kaya<sup>1</sup>

<sup>1</sup>Department of Electrical and Electronics Engineering, Bülent Ecevit University, İnceviz, Zonguldak, Turkey

 E-mail: f.kara@beun.edu.tr

**Abstract:** Non-orthogonal multiple access (NOMA) is a strong candidate for next generation radio access networks due to its ability of serving multiple users using the same time and frequency resources. Therefore, researchers in academia and industry have been recently investigating the error performances and capacity of NOMA schemes. The main drawback of NOMA techniques is the interference among users due to the its non-orthogonal access nature, that is usually solved by interference cancellation techniques such as successive interference cancellation (SIC) at the receivers. On the other hand, the interference among users may not be completely eliminated in the SIC process due to the erroneous decisions in the receivers usually caused by channels. In this study, for the first time in the literature, the authors derive an exact closed-form bit error rate (BER) expressions under SIC error for downlink NOMA over Rayleigh fading channels. Besides, they derive one-degree integral form exact BER expressions and closed-form approximate expressions for uplink NOMA. Then, the derived expressions are validated by simulations. The numerical results are depicted to reveal the effects of error during SIC process on the performance for various cases such as power allocation for downlink and channel quality difference for uplink.

## 1 Introduction

The future radio access networks (5G and beyond) are to support very high rate, ultra-low latency, massive connections and very high mobility applications [1, 2]. To fulfil these targets, non-orthogonal multiple access (NOMA) is highly recommended and investigated by the researchers. NOMA achieves high spectral efficiency and supports dense networks by allowing the users to share same radio resources [3]. The conventional orthogonal multiple access (OMA) schemes serve to the multiple users by assigning them into different radio resources, e.g. frequency and time. In contrast to OMA, NOMA simultaneously serves multiple user equipments on the same resource blocks by splitting users into power domain. This NOMA principle is based on superposition coding (SC) at the transmitter and successive interference cancellation (SIC) at the receivers [4, 5].

In [6], researchers first proposed the NOMA for future cellular network and demonstrated its potential in terms of capacity and user-fairness compared to OMA schemes. Due to this potential, NOMA has been studied largely in the last years in terms of outage performance [7–10], power allocation [11–13], user clustering [13–15] and system capacity [16, 17]. Most of these studies approach all these problems by considering Shannon capacity theorem. The outage performances are obtained by comparing the targeted data rates (quality of service) of users with the achievable maximum Shannon rate. Also, the power allocation and user clustering algorithms are based on maximising this achievable Shannon rate. However, researchers mostly assume that the SIC process is error free. This assumption is not reasonable for the wireless communication. Only in a few studies, the error during the SIC is regarded. Bit error rate (BER) performance with the proposed triangle-SIC error is investigated on an asynchronous uplink NOMA (UL-NOMA) scheme in [18] where BER performances are given with the sum of permutations. In [19], BER expressions for UL-NOMA with the SIC error are obtained over additive white Gaussian noise (AWGN) channel. However, the channel coefficients are assumed as constants not a random variable, so the derived closed-form equation does not include the effects of random fading. For uplink, uncoded-NOMA and coded-NOMA BER performances are only investigated via simulations in [20]. In [21], BER performances of downlink NOMA (DL-NOMA) are

investigated with the perfect and imperfect SIC by simulations, no analytical derivation and result are given.

In addition to conventional NOMA systems, the NOMA with the other physical layer techniques such as multiple-input multiple-output (MIMO) [22, 23] and cooperative communication [24–29] are also proposed in the literature. However, in those NOMA involved system models, the performances have been only studied in terms of outage probability and overall system capacity. The derivation for the BER of the systems has been not given in the literature.

To the best of authors' knowledge, there is no analytical BER derivation in the literature for NOMA in the presence of SIC errors over fading channels. In this paper, for the first time in the literature, closed-form exact BER expressions for DL-NOMA are derived in the presence of SIC errors over Rayleigh fading channels. On the other hand, the exact BER expressions over Rayleigh fading channel for UL-NOMA could only be obtained in a single-integral form. Nevertheless, the approximate closed-form BER for the UL-NOMA is derived. Furthermore, the probability density function (PDF) of the difference of two independent and non-identically distributed (i.n.i.d) Rayleigh distributions is derived first in the literature to the best of authors' knowledge. The analytical results are verified with the simulations. The analytical results obtained in this paper can be extended for more complex NOMA models such as MIMO-NOMA [22, 23], cooperative NOMA [24] and relay-aided NOMA [25–29]. However such analyses are left for future works, since they are beyond the scope of this paper.

The rest of paper is organised as follows. In Section 2, the system models of DL-NOMA and UL-NOMA are introduced. In Section 3, exact error probability expressions are derived for both DL-NOMA and UL-NOMA. Also, approximate error probability expressions are presented for UL-NOMA in this section. Then, the analytical and Monte-Carlo simulation results are presented for the different scenarios in Section 4. Finally, in Section 5 the results are discussed and the paper is concluded.

## 2 System model

### 2.1 Downlink NOMA

This paper considers the DL-NOMA scenario with two users and one base station (BS). The BS transmits signals of users on the same frequency and time slots by using SC. SC is implemented at the BS by summing signals of users after multiplying them with the different power coefficients. It is assumed that all nodes have a single antenna. The system model for DL-NOMA is shown in Fig. 1a. The received signal by the users is given as

$$y_k = h_k x_{sc} + w_k, \quad k = 1, 2 \quad (1)$$

where  $h_k$  is the channel coefficient for  $k$ th user.  $h_k$  denotes i.n.i.d Rayleigh fading channel coefficients between BS and users.  $w_k$  is the AWGN at each users' receiver, respectively.  $w_k$  has zero mean and  $N_0/2$  variance.  $x_{sc}$  is the superposition coded signal at BS and is defined as

$$x_{sc} = \sqrt{\epsilon_1}x_1 + \sqrt{\epsilon_2}x_2, \quad (2)$$

where  $\epsilon_1$  and  $\epsilon_2$  denote the symbols energies of the users. They are given as  $\epsilon_1 = \alpha P_s$ ,  $\epsilon_2 = (1 - \alpha)P_s$ , respectively.  $x_1$ ,  $x_2$  are modulated symbols of users.  $P_s$  is the transmit power of BS. It is assumed that  $|h_1|^2 > |h_2|^2$ . Therefore, user1 and user2 represent the intra-cell user (near user – NU) and cell-edge user (far user – FU), respectively. The total transmit power is allocated to the symbols of users with the power coefficient  $\alpha$ .

Generally, a high modulation level is selected in case of a high channel quality, whereas a low modulation level is selected in case of a poor channel quality to sustain a reliable BER performance. In a NOMA scheme, FUs experience more severe channel conditions than NUS, hence a BPSK modulation is selected for the FU, while QPSK modulation for the NU is selected for the sake of simplicity in the description of the detection/decision process. Nevertheless, higher order modulations than QPSK can be also employed in our derivations.

FU detects own symbols from the received  $y_2$  signal by using maximum-likelihood (ML) detector pretending the NU signals as interference. On the other hand, NU detects own symbols by using the SIC process. First, NU detects the FU symbol like as its own signal is noise then it subtracts regenerated FU symbol from the received  $y_1$  and detects its own symbol. If the NU detects the symbols of FU correctly, it can decode its own symbols correctly with high probability. However, if the error happens when detecting FU symbols during the SIC, it gives rise to detecting NU own symbols erroneously. This SIC error phoneme depends on the mostly channel coefficients and the power allocation coefficient.

### 2.2 Uplink NOMA

The UL-NOMA scenario is considered with two users and one BS similar to DL-NOMA. The users transmit their signals by their own transmit powers on the same time and frequency blocks. The BS implements SIC after receiving the total signal. It is assumed that all nodes have a single antenna. The system model is shown in Fig. 1b. The received signal at the BS is defined as follows:

$$y = \sqrt{P_1}h_1x_1 + \sqrt{P_2}h_2x_2 + w, \quad (3)$$

where  $P_i$  and  $h_i$  denote the transmit powers of users, independent and non-identical Rayleigh fading channel coefficients between users and BS, respectively.  $w$  is the AWGN with zero ('0') mean and  $N_0/2$  variance.  $x_1$  and  $x_2$  are the QPSK and BPSK modulated symbols of users. It is assumed that  $|h_1|^2 > |h_2|^2$ . Hence, user1 and user2 denote the intra-cell user (NU) and cell-edge user (FU), respectively. Owing to better channel condition, NU symbols are detected first during the SIC implemented at BS. FU symbols are detected after subtracting the detected NU symbols from  $y$ . As explained in the downlink scenario, the SIC error from the NU

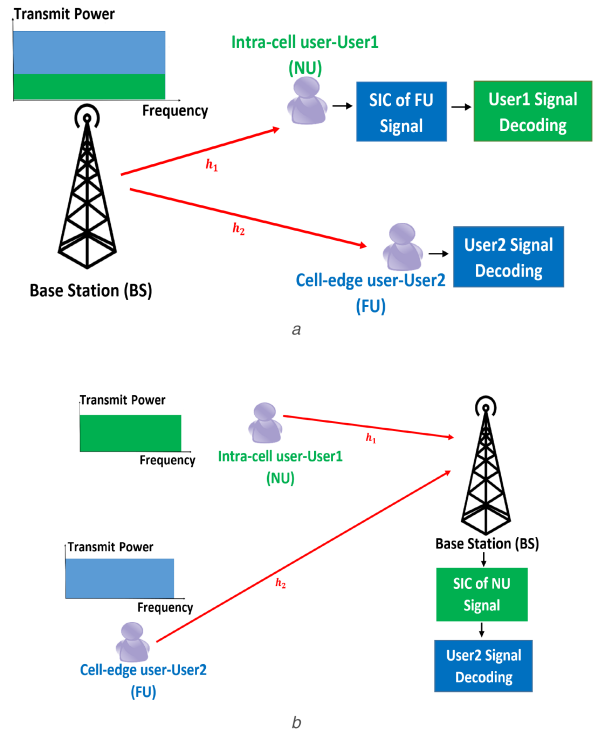


**Fig. 1** Illustrations of NOMA systems

- (a) Downlink,
- (b) Uplink

drives the error performance of FU. This SIC error depends on the channel qualities and the difference of the transmit powers of users.

## 3 BER analyses

In this section, exact BER expressions are analysed first for DL-NOMA, then for UL-NOMA. Approximate BER expressions are presented for UL-NOMA.

In the rest of section, the used notations are as follows:  $P_r(\varphi)$  denotes the probability of  $\varphi$  event.  $P_k(e)$  denotes the bit error probability of  $k$ th user. Additionally,  $P(e|\vartheta)$  denotes the bit error probability under the condition that  $\vartheta$  is happened. Finally,  $\overline{P_k(e)}$  denotes the average bit error probability.

### 3.1 Exact BER expression for DL-NOMA

The received signal constellation at users is given in Fig. 2a. In Fig. 2a, user1 and user2 symbols are shown in the form of  $[x_1, x_2]$ . The binary bit representations for two users are given in the form of  $[i_{1,2}, i_{1,2}]$  in Fig. 2, where the first digit of the sub-index represents the user, the second one represents the bit order.

NU first detects FU symbols and after subtracting detected FU symbols SIC detects its own symbols. On the other hand, the decoding process at the FU is implemented by pretending the NU symbols as noise. Hence, FU decides directly its own symbols according to received superposition coded symbols. This decision is held according to ML detection. The ML decision boundaries in Figs. 2 and 3 are defined according to the ML detecting rule. The decision for a received symbol is based on the constellation region to which the received signal belongs. Since a BPSK modulation is employed for FU, the decision boundary is based on whether the in-phase component of the received signal is higher than zero or lower and equal to zero ( $y_I > 0$  or  $y_I \leq 0$ ). On the other hand, the decision for the NU is performed according to the four regions since QPSK modulation is used. Therefore, the decision boundary for the NU is based on whether the both real and imaginary parts of received signal are higher than zero or lower and equal to zero (i.e.  $y_I > 0$  and  $y_Q > 0$ ,  $y_I > 0$  and  $y_Q \leq 0$ ,  $y_I \leq 0$  and  $y_Q > 0$  or  $y_I \leq 0$  and  $y_Q \leq 0$  where  $y_I$  and  $y_Q$  are the real and imaginary components of received signal, respectively).

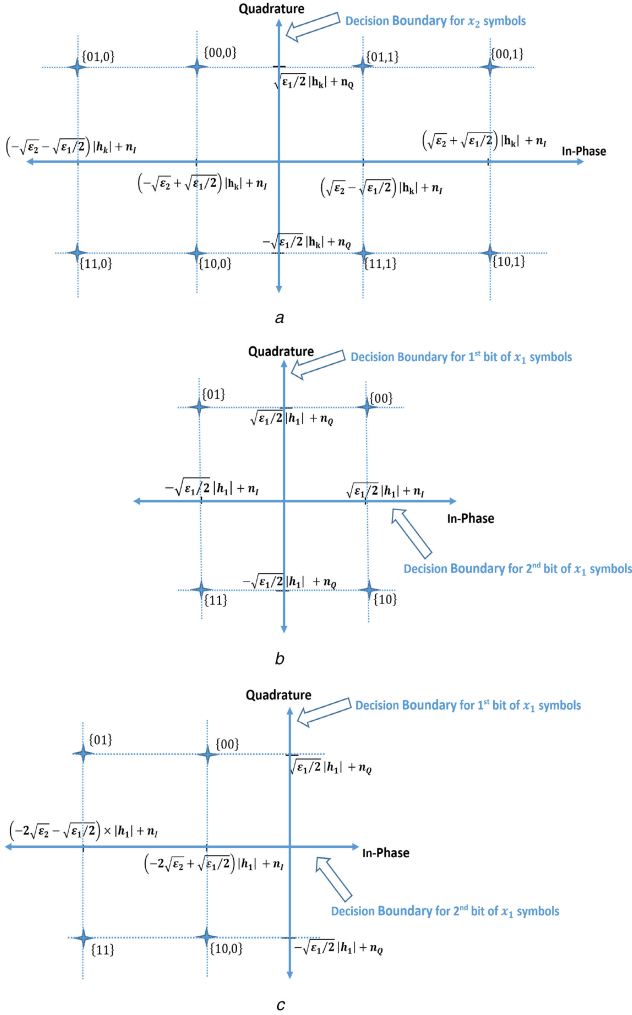


**Fig. 2** Received signal spaces of DL-NOMA

- (a) Signal space received by users for DL-NOMA,
- (b) Signal space of NU user after subtracting FU symbol detected correctly,
- (c) Signal space of NU user after subtracting FU symbol detected erroneously

In order to derive BER of FU symbols, the channel coefficient given in Fig. 2a is taken as  $h_2$  in the received signal space as defined in (1). The error probability of ML detector is defined as the sum of error probability of each possible symbol (different point in the constellation) multiplied by the prior probability of that symbol. We assume that all  $x_1$  and  $x_2$  symbols have equal prior probability. Hence, the prior probabilities of all  $x_{sc}$  symbols given in Fig. 2a are equal (i.e. 1/8). The erroneous decision of any  $x_{sc}$  symbol only may occur when the AWGN cause the received symbol to cross other regions of the decision boundary. For instance, we assume that  $x_{sc} = \{10, 0\}$  symbol is sent as superposition coded. According to the decision boundary given in Fig. 2a for FU symbols, this  $x_{sc}$  symbol is detected erroneously if only the in-phase component of AWGN is higher than the in-phase component of this symbol's amplitude ( $n_i \geq \sqrt{\varepsilon_2} h_2 - \sqrt{\varepsilon_1/2} h_2$ ).

By considering the ML detection rule, the error probabilities of each  $x_{sc}$  symbol could be easily obtained. By multiplying these error probabilities of each  $x_{sc}$  symbol with the prior probability of that  $x_{sc}$  symbol, the error probability at FU can be defined as

$$P_2(e) = \frac{1}{2} \left[ P_r \left( n_i \geq \sqrt{\varepsilon_2} h_2 + \sqrt{\frac{\varepsilon_1}{2}} h_2 \right) + P_r \left( n_i \geq \sqrt{\varepsilon_2} h_2 - \sqrt{\frac{\varepsilon_1}{2}} h_2 \right) \right]. \quad (4)$$

The received signal is exposed to an AWGN in both in-phase ( $n_i$ ) and quadrature ( $n_Q$ ) components as shown in Fig. 2. However,

the quadrature noise component  $n_Q$  has no effect on the decision of the symbols for FU, since the decision variable for the received signal as it is higher than zero or lower and equal to zero ( $y_i > 0$  or  $y_i \leq 0$ ). Consequently, the expression of the error probability in (4) only includes the in-phase noise component  $n_i$ .

The error probability given in (4) can be defined as

$$P_2(e) = \frac{1}{2} \left[ Q \left( \frac{(\sqrt{\varepsilon_2} + \sqrt{\varepsilon_1/2}) h_2}{\sqrt{N_0}/2} \right) + Q \left( \frac{(\sqrt{\varepsilon_2} - \sqrt{\varepsilon_1/2}) h_2}{\sqrt{N_0}/2} \right) \right]. \quad (5)$$

To make the paper easy to follow and to avoid using long expressions inside the functions, simple notations are defined in the following of this paper. For this reason, the expressions inside the  $Q(\cdot)$  functions in (5) can be defined as

$$\begin{aligned} \gamma_A &= \frac{(\sqrt{2\varepsilon_2} + \sqrt{\varepsilon_1})^2 |h_2|^2}{N_0}, & \bar{\gamma}_A &= \frac{(\sqrt{2\varepsilon_2} + \sqrt{\varepsilon_1})^2}{N_0} E[|h_2|^2], \\ \gamma_B &= \frac{(\sqrt{2\varepsilon_2} - \sqrt{\varepsilon_1})^2 |h_2|^2}{N_0}, & \bar{\gamma}_B &= \frac{(\sqrt{2\varepsilon_2} - \sqrt{\varepsilon_1})^2}{N_0} E[|h_2|^2]. \end{aligned} \quad (6)$$

In (6),  $E[\cdot]$  is the expectation operator. Besides notations,  $\gamma_A$  and  $\gamma_B$  are the signal-to-noise ratios (SNRs) for the different signal constellation points given in Fig. 2a.  $\gamma_A$  and  $\gamma_B$  represent the in-phase components of SNR for the  $x_{sc} = \{01, 0\}, \{11, 0\}, \{00, 1\}, \{10, 1\}$  and for the  $x_{sc} = \{00, 0\}, \{10, 0\}, \{01, 1\}, \{11, 1\}$  symbols, respectively. This consideration will be also valid for the similar notation definitions in the following of the paper. By substituting (6) into (5), the probability error is obtained as

$$P_2(e) = \frac{1}{2} [Q(\sqrt{\gamma_A}) + Q(\sqrt{\gamma_B})]. \quad (7)$$

Then, the average BER at FU can be obtained as

$$\overline{P_2(e)} = \frac{1}{2} \left[ \int_0^\infty Q(\sqrt{\gamma_A}) f_{\gamma_A}(\gamma_A) d\gamma_A + \int_0^\infty Q(\sqrt{\gamma_B}) f_{\gamma_B}(\gamma_B) d\gamma_B \right]. \quad (8)$$

In case of a Rayleigh fading channel, the channel coefficient  $h_k$  has PDF of Rayleigh distribution, hence, the PDF of SNR is defined as

$$f_{\gamma_i}(\gamma) = \frac{1}{\bar{\gamma}_i} e^{-\gamma/\bar{\gamma}_i}, \quad \gamma \geq 0, \quad i = A, B. \quad (9)$$

By using alternative representation of  $Q$  function defined by Craig [[30], Eq. (9)] and moment generating function (MGF) definition [[31], Eq. (17)], the average BER expression at FU is given as

$$\overline{P_2(e)} = \frac{1}{2} \left[ \frac{1}{\pi} \int_0^{\pi/2} MGF_{\gamma_A} \left( \frac{1}{\sin^2 \theta} \right) d\theta + \frac{1}{\pi} \int_0^{\pi/2} MGF_{\gamma_B} \left( \frac{1}{\sin^2 \theta} \right) d\theta \right], \quad (10)$$

where

$$MGF_{\gamma_i}(s) = \frac{1}{1 + s\bar{\gamma}_i}, \quad i = A, B. \quad (11)$$

With the aid of [[32], Eq. (5.6)], by substituting (11) into (10), the error probability of the FU becomes

$$\overline{P_2(e)} = \frac{1}{4} \left[ \left( 1 - \sqrt{\frac{\gamma_A}{2 + \gamma_A}} \right) + \left( 1 - \sqrt{\frac{\gamma_B}{2 + \gamma_B}} \right) \right]. \quad (12)$$

On the other hand, the error probability of NU has to be handled differently because of the SIC process and its error. The total error probability of NU is given as the sum of the two different cases in which FU symbols are detected correctly or erroneously during the SIC process. Hence

$$P_1(e) = P_1(e|\text{correct}_{\text{FU}}) + P_1(e|\text{error}_{\text{FU}}), \quad (13)$$

where  $P_1(e|\text{correct}_{\text{FU}})$  is the probability under the condition that no error occurred when detecting FU symbols at NU.  $P_1(e|\text{error}_{\text{FU}})$  is the probability under the condition that error occurred when detecting FU symbols at NU.

The constellation maps for NU after the SIC process are shown in Fig. 2 for two cases that are FU symbols and are detected correctly or erroneously. The decision boundaries of the ML for the QPSK demodulation are shown in Fig. 2b and c. In Fig. 2b, it is assumed that FU symbols are detected correctly and subtracted from the total received signal. In this case, only NU symbols ( $x_1$ ) with the fading and the AWGN remain. However, the priori probabilities of NU symbols depend on the correct-decoded FU ( $x_2$ ) symbols during the SIC process. Hence, the probability of correct decoding  $x_2$  for different  $x_{sc}$  symbols should be considered. These priori probabilities, the probabilities of correct detected FU symbol at NU, can be easily obtained by considering the ML detection boundary for FU symbols given in Fig. 2a as in (4). Then, the error probability of each NU symbol ( $x_1$ ) given in Fig. 2b can be obtained according to the ML detection boundary of QPSK.

The BER of QPSK modulation is obtained by averaging the error probability of two bits (i.e.  $i_{1,1}$  and  $i_{1,2}$ ). Since Gray mapping is used for NU symbols, a wrong decision of the NU symbols causes a single bit error. Hence, the bit error probability of NU, under the condition that no error occurred when detecting FU symbols, is given as

$$\begin{aligned} P_1(e|\text{correct}_{\text{FU}}) &= \frac{1}{2} \left[ \frac{1}{2} P_r \left( n_1 \leq \sqrt{\epsilon_2} h_1 - \sqrt{\frac{\epsilon_1}{2}} h_1 \right) \right. \\ &\quad \times \left\{ P_r \left( n_1 \leq -\sqrt{\frac{\epsilon_1}{2}} h_1 \middle| n_1 \leq \sqrt{\epsilon_2} h_1 - \sqrt{\frac{\epsilon_1}{2}} h_1 \right) \right. \\ &\quad + P_r \left( n_Q \geq \sqrt{\frac{\epsilon_1}{2}} h_1 \middle| n_1 \leq \sqrt{\epsilon_2} h_1 - \sqrt{\frac{\epsilon_1}{2}} h_1 \right) \Big\} \\ &\quad + \frac{1}{2} P_r \left( n_1 \leq \sqrt{\epsilon_2} h_1 + \sqrt{\frac{\epsilon_1}{2}} h_1 \right) \\ &\quad \times \left\{ P_r \left( n_1 \geq \sqrt{\frac{\epsilon_1}{2}} h_1 \middle| n_1 \leq \sqrt{\epsilon_2} h_1 + \sqrt{\frac{\epsilon_1}{2}} h_1 \right) \right. \\ &\quad \left. \left. + P_r \left( n_Q \geq \sqrt{\frac{\epsilon_1}{2}} h_1 \middle| n_1 \leq \sqrt{\epsilon_2} h_1 + \sqrt{\frac{\epsilon_1}{2}} h_1 \right) \right\} \right]. \end{aligned} \quad (14)$$

where  $\frac{1}{2} P_r(n_1 \leq \sqrt{\epsilon_2} h_1 - \sqrt{\epsilon_1/2} h_1)$  and  $\frac{1}{2} P_r(n_1 \leq \sqrt{\epsilon_2} h_1 + \sqrt{\epsilon_1/2} h_1)$  are the priori probabilities that are likely the error probabilities of the FU given as (4), when the channel coefficient is taken as  $h_1$  in Fig. 2a. The only difference is that the probabilities define the correct decoding (the noise is lower than the signal level). The second and third terms in the (14) are the error probabilities of first and second bits for  $x_1 = \{01\}$  or  $\{11\}$  symbols, respectively. The fifth and sixth terms are the error probabilities of first and second bits for the remaining of  $x_1$  symbols. All these definitions are conditional because this situation is under the condition that FU symbols ( $x_2$ ) are detected correctly. The condition expressions define the situation at which a correct decoding is performed.

The probability of an  $A$  event under the condition an  $B$  event is given as

$$P(A|B) = \frac{P(A \cap B)}{P(B)}. \quad (15)$$

With the aid of (15), the error probability of NU under the assumption that FU symbols detected correctly can be redefined as

$$\begin{aligned} P_1(e|\text{correct}_{\text{FU}}) &= \frac{1}{4} \left[ P_r \left( n_1 \leq -\sqrt{\frac{\epsilon_1}{2}} h_1 \right) \right. \\ &\quad + P_r \left( \sqrt{\frac{\epsilon_1}{2}} h_1 \leq n_1 \leq \sqrt{\epsilon_2} h_1 + \sqrt{\frac{\epsilon_1}{2}} h_1 \right) \\ &\quad + P_r \left( n_Q \geq \sqrt{\frac{\epsilon_1}{2}} h_1 \right) \times \left\{ P_r \left( n_1 \leq \sqrt{\epsilon_2} h_1 - \sqrt{\frac{\epsilon_1}{2}} h_1 \right) \right. \\ &\quad \left. \left. + P_r \left( n_1 \leq \sqrt{\epsilon_2} h_1 + \sqrt{\frac{\epsilon_1}{2}} h_1 \right) \right\} \right]. \end{aligned} \quad (16)$$

Since the writing the above  $P_1$  error expression in terms of  $Q(\cdot)$  functions will create a huge expression, for the sake of simplicity we define

$$\begin{aligned} \gamma_C &= \frac{\epsilon_1 \times |h_1|^2}{N_0}, \quad \bar{\gamma}_C = \frac{\epsilon_1}{N_0} E[|h_1|^2], \\ \gamma_D &= \frac{(\sqrt{2\epsilon_2} + \sqrt{\epsilon_1})^2 |h_1|^2}{N_0}, \quad \bar{\gamma}_D = \frac{(\sqrt{2\epsilon_2} + \sqrt{\epsilon_1})^2}{N_0} E[|h_1|^2], \\ \gamma_E &= \frac{(\sqrt{2\epsilon_2} - \sqrt{\epsilon_1})^2 |h_1|^2}{N_0}, \quad \bar{\gamma}_E = \frac{(\sqrt{2\epsilon_2} - \sqrt{\epsilon_1})^2}{N_0} E[|h_1|^2]. \end{aligned} \quad (17)$$

Then, the error probability of NU under the condition that FU symbols are detected correctly, in terms of the above defined SNRs within  $Q(\cdot)$  functions becomes

$$\begin{aligned} P_1(e|\text{correct}_{\text{FU}}) &= \frac{1}{4} [Q(\sqrt{\gamma_C}) \times \{4 - Q(\sqrt{\gamma_D}) \\ &\quad - Q(\sqrt{\gamma_E})\} - Q(\sqrt{\gamma_D})]. \end{aligned} \quad (18)$$

In Fig. 2c, the constellation map at the NU, after subtracting FU symbols detected erroneously, is given. It is assumed that,  $x_2 = 1\{i_2 = 1\}$  symbol is sent by transmitter and it is detected erroneously as  $x_2 = -1\{i_2 = 0\}$ . As the FU symbols have an equal prior probability, the constellation map will be similar vice versa. However, the points in the signal space under the condition that FU symbols detected erroneously do not have equal priori probabilities. These priori probabilities depend on that which  $x_{sc}$  symbols was/were sent. Therefore, it should be taken into consideration that which  $x_{sc}$  symbol is sent, under the condition of  $x_2$  symbols are detected erroneously. By considering this, the priori probabilities for different  $x_1$  symbols are obtained similar to (14) by using (4). Also, the error probabilities of each  $x_1$  symbols are defined in the form of conditional probabilities similar to (14) by considering ML detection rule, signal constellation and QPSK decision boundaries given in Fig. 2c. As a result of this, the error probability of NU symbols, under the assumption of FU symbols detected erroneously, is defined as follows: (see (19)). In (19), the first and fourth terms are the priori probabilities of the  $x_2$  symbols detected erroneously. The second and fifth terms are the error probabilities of the first bits, and lastly, the third and sixth terms are the error probabilities of the second bits of the  $x_1$  symbols. The conditions define the events that the FU symbols ( $x_2$ ) are detected erroneously for those symbols.

By using (15), the error probability for NU, in case of the FU symbols are detected erroneously, is given as

$$\begin{aligned} P_1(e|\text{error}_{\text{FU}}) &= \frac{1}{4} \left[ P_r \left( \sqrt{\epsilon_2} h_1 - \sqrt{\frac{\epsilon_1}{2}} h_1 \leq n_1 \leq 2\sqrt{\epsilon_2} h_1 - \sqrt{\frac{\epsilon_1}{2}} h_1 \right) \right. \\ &\quad + P_r \left( n_1 \geq 2\sqrt{\epsilon_2} h_1 + \sqrt{\frac{\epsilon_1}{2}} h_1 \right) \\ &\quad + P_r \left( n_Q \geq \sqrt{\frac{\epsilon_1}{2}} h_1 \right) \times \left\{ P_r \left( n_1 \geq \sqrt{\epsilon_2} h_1 - \sqrt{\frac{\epsilon_1}{2}} h_1 \right) \right. \\ &\quad \left. \left. + P_r \left( n_1 \geq \sqrt{\epsilon_2} h_1 + \sqrt{\frac{\epsilon_1}{2}} h_1 \right) \right\} \right]. \end{aligned} \quad (20)$$

$$\begin{aligned}
P_1(e|\text{error}_{\text{FU}}) = & \frac{1}{2} \left[ \frac{1}{2} P_r \left( n_1 \geq \sqrt{\varepsilon_2} h_1 - \sqrt{\frac{\varepsilon_1}{2}} h_1 \right) \right. \\
& \times \left\{ P_r \left( n_1 \leq 2\sqrt{\varepsilon_2} h_1 - \sqrt{\frac{\varepsilon_1}{2}} h_1 \middle| n_1 \geq \sqrt{\varepsilon_2} h_1 - \sqrt{\frac{\varepsilon_1}{2}} h_1 \right) \right. \\
& + P_r \left( n_1 \geq \sqrt{\frac{\varepsilon_1}{2}} h_1 \middle| n_1 \geq \sqrt{\varepsilon_2} h_1 - \sqrt{\frac{\varepsilon_1}{2}} h_1 \right) \Big] \\
& + \frac{1}{2} P_r \left( n_1 \geq \sqrt{\varepsilon_2} h_1 + \sqrt{\frac{\varepsilon_1}{2}} h_1 \right) \times \\
& \left\{ P_r \left( n_1 \geq 2\sqrt{\varepsilon_2} h_1 + \sqrt{\frac{\varepsilon_1}{2}} h_1 \middle| n_1 \geq \sqrt{\varepsilon_2} h_1 + \sqrt{\frac{\varepsilon_1}{2}} h_1 \right) \right. \\
& \left. \left. + P_r \left( n_1 \geq \sqrt{\frac{\varepsilon_1}{2}} h_1 \middle| n_1 \geq \sqrt{\varepsilon_2} h_1 + \sqrt{\frac{\varepsilon_1}{2}} h_1 \right) \right\}. \right]
\end{aligned} \tag{19}$$

In order to simplify the above expression in terms of  $Q(\cdot)$  functions, we define the SNRs as

$$\begin{aligned}
\gamma_F &= \frac{(2\sqrt{2\varepsilon_2} + \sqrt{\varepsilon_1})^2 |h_1|^2}{N_0}, \quad \bar{\gamma}_F = \frac{(2\sqrt{2\varepsilon_2} + \sqrt{\varepsilon_1})^2}{N_0} E[|h_1|^2], \\
\gamma_G &= \frac{(2\sqrt{2\varepsilon_2} - \sqrt{\varepsilon_1})^2 |h_1|^2}{N_0}, \quad \bar{\gamma}_G = \frac{(2\sqrt{2\varepsilon_2} - \sqrt{\varepsilon_1})^2}{N_0} E[|h_1|^2].
\end{aligned} \tag{21}$$

Then, the error probability of NU, when FU symbols are detected erroneously, turns out to be

$$\begin{aligned}
P_1(e|\text{error}_{\text{FU}}) = & \frac{1}{4} [Q(\sqrt{\gamma_C}) \times \{Q(\sqrt{\gamma_D}) + Q(\sqrt{\gamma_E})\} \\
& + Q(\sqrt{\gamma_E}) + Q(\sqrt{\gamma_F}) - Q(\sqrt{\gamma_G})].
\end{aligned} \tag{22}$$

By summing of (18) and (22), the total error probability of NU can be written as

$$\begin{aligned}
P_1(e) = & Q(\sqrt{\gamma_C}) + \frac{1}{4} [-Q(\sqrt{\gamma_D}) \\
& + Q(\sqrt{\gamma_E}) + Q(\sqrt{\gamma_F}) - Q(\sqrt{\gamma_G})].
\end{aligned} \tag{23}$$

Then, the total average BER of NU is calculated by averaging the above expression over the random SNR values, and becomes

$$\begin{aligned}
\overline{P_1(e)} = & \int_0^\infty Q(\sqrt{\gamma_C}) f_{\gamma_C}(\gamma_C) d\gamma_C + \frac{1}{4} \\
& \times \left[ - \int_0^\infty Q(\sqrt{\gamma_D}) f_{\gamma_D}(\gamma_D) d\gamma_D + \int_0^\infty Q(\sqrt{\gamma_E}) f_{\gamma_E}(\gamma_E) d\gamma_E \right. \\
& \left. + \int_0^\infty Q(\sqrt{\gamma_F}) f_{\gamma_F}(\gamma_F) d\gamma_F - \int_0^\infty Q(\sqrt{\gamma_G}) f_{\gamma_G}(\gamma_G) d\gamma_G \right]. \tag{24}
\end{aligned}$$

Again by utilising [[32], Eq. (5.6)], the total average BER of NU is derived as

$$\begin{aligned}
\overline{P_1(e)} = & \frac{1}{2} \left( 1 - \sqrt{\frac{\bar{\gamma}_C}{2 + \bar{\gamma}_C}} \right) + \frac{1}{8} \left[ \sqrt{\frac{\bar{\gamma}_D}{2 + \bar{\gamma}_D}} \right. \\
& \left. - \sqrt{\frac{\bar{\gamma}_E}{2 + \bar{\gamma}_E}} + \sqrt{\frac{\bar{\gamma}_F}{2 + \bar{\gamma}_F}} - \sqrt{\frac{\bar{\gamma}_G}{2 + \bar{\gamma}_G}} \right]. \tag{25}
\end{aligned}$$

### 3.2 Exact BER expressions for UL-NOMA

The received signal at BS for UL-NOMA is given in (3). To detect both users' symbols, SIC is implemented at BS as NU for DL-NOMA. Hence, a similar method applied to NU for DL-NOMA can be followed to obtain exact error performances of users for UL-NOMA. However, there are distinct differences such that users' symbols encounter different channel conditions and decoding order is reverse. Due to  $|h_1|^2 > |h_2|^2$ , BS detects first the  $x_1$  symbols. Then, it subtracts regenerated  $\tilde{x}_1$  symbols from the received signal and detects the  $x_2$  symbols. The received signal space at the BS is given

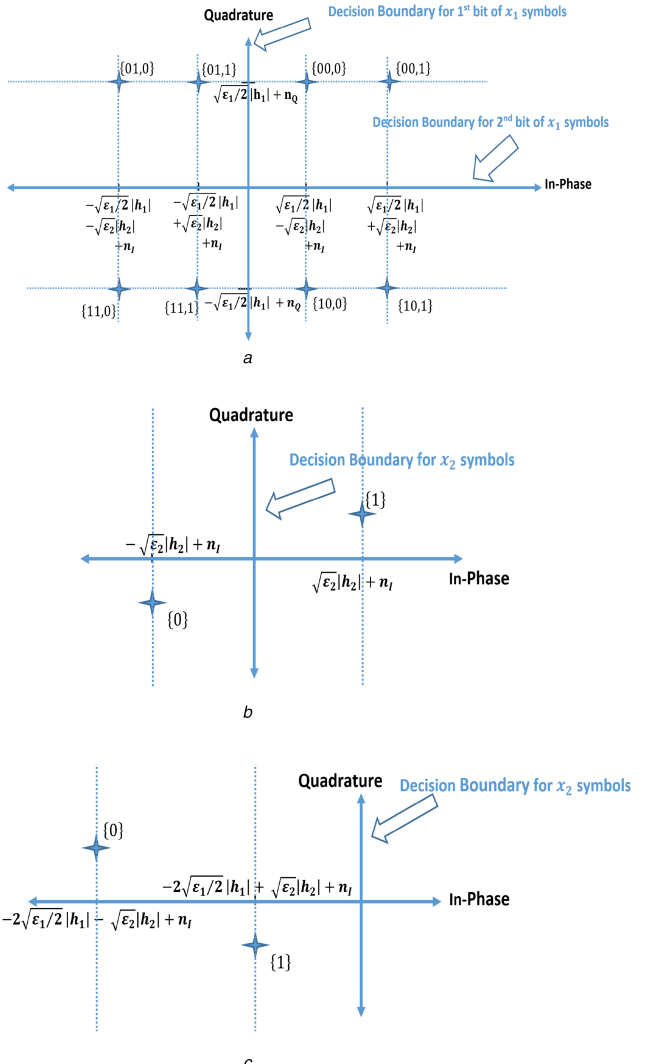


**Fig. 3** Received signal spaces of UL-NOMA

- (a) Signal space received by BS for UL-NOMA,
- (b) Signal space of FU user after subtracting NU symbol when first bit detected correctly,
- (c) Signal space of FU user after subtracting NU symbol when first bit detected erroneously

in Fig. 3a on the scenario NU symbols are modulated by QPSK and FU symbols are modulated by BPSK for UL-NOMA. In Fig. 3a, user1 and user2 symbols are shown in the form of  $x_1, x_2$ . The ML decision boundaries of QPSK for NU symbols are shown in Fig. 3a.

We assume that all  $x_1$  and  $x_2$  symbols have an equal priori probability. The total error probability of the NU is defined as the sum of error probabilities of each possible symbols multiplied with

the priori probability of the symbol like as the DL scenario given in (4). Hence, by considering the signal constellation and the decision boundaries given in Fig. 3a, the bit error probability of NU can be defined as

$$\begin{aligned} P_1(e) = & \frac{1}{2} \left[ P_r \left( n_0 \geq \sqrt{\frac{\epsilon_1}{2}} h_1 \right) \right. \\ & + \frac{1}{2} \left\{ P_r \left( n_1 \geq \sqrt{\frac{\epsilon_1}{2}} h_1 + \sqrt{\epsilon_2} h_2 \right) \right. \\ & \left. \left. + P_r \left( n_1 \geq \sqrt{\frac{\epsilon_1}{2}} h_1 - \sqrt{\epsilon_2} h_2 \right) \right\}. \right] \end{aligned} \quad (26)$$

The first and second terms in (26) are the error probabilities of first bits of  $x_1$  symbols and the third term is the error probability of second bits of  $x_1$  symbols. Consequently, the error probability in (26) can be expressed as

$$P_1(e) = \frac{1}{2} \left[ Q \left( \sqrt{\frac{\epsilon_1 |h_1|^2}{N_0}} \right) + \frac{1}{2} \{ Q(z) + Q(w) \} \right], \quad (27)$$

where  $z$  and  $w$  are random variables and defined as

$$\begin{aligned} z &= \sqrt{\frac{\epsilon_1}{N_0}} h_1 + \sqrt{\frac{2\epsilon_2}{N_0}} h_2, \\ w &= \sqrt{\frac{\epsilon_1}{N_0}} h_1 - \sqrt{\frac{2\epsilon_2}{N_0}} h_2. \end{aligned} \quad (28)$$

In case of a Rayleigh channel, hence both channel coefficients  $h_1$  and  $h_2$  have PDF of Rayleigh distribution, the PDF for sum of independent non-identical Rayleigh distributions is given in [[33], Eq. (8)] as

$$\begin{aligned} f_Z(z) = & \frac{a_1^2 z}{(a_1^2 + a_2^2)^2} \exp \left( -\frac{z^2}{2a_1^2} \right) + \frac{a_2^2 z}{(a_1^2 + a_2^2)^2} \exp \left( -\frac{z^2}{2a_2^2} \right) \\ & + \sqrt{\frac{\pi a_1 a_2 [z^2 - (a_1^2 + a_2^2)]}{(a_1^2 + a_2^2)^2}} \exp \left( -\frac{z^2}{2(a_1^2 + a_2^2)} \right) \\ & \left[ \operatorname{erf} \left( \frac{za_2}{a_1 \sqrt{2(a_1^2 + a_2^2)}} \right) + \operatorname{erf} \left( \frac{za_1}{a_2 \sqrt{2(a_1^2 + a_2^2)}} \right) \right], \end{aligned} \quad (29)$$

where  $\operatorname{erf}(.)$  is the error function and  $\operatorname{erf}(x) = 2/\sqrt{\pi} \int_0^x e^{-t^2} dt$ . In our case,  $a_1 = \sqrt{\epsilon_1/2N_0 E[|h_1|^2]}$ ,  $a_2 = \sqrt{\epsilon_2/N_0 E[|h_2|^2]}$  are defined.

The PDF for the difference of two independent non-identical Rayleigh distributions is written as (see appendix for derivation)

$$\begin{aligned} f_W(w) = & \frac{4e^{-w^2/\Omega_X}}{\Omega_X \Omega_Y} \left[ \frac{\sqrt{\pi} \operatorname{erfc} \left( \frac{w(1-\tau\Omega_X)}{\sqrt{\tau}\Omega_X} \right) \exp \left( \frac{w^2}{\tau\Omega_X^2} \right)}{2\tau^{\frac{3}{2}}\Omega_X} \times \right. \\ & \left. \left\{ \frac{\tau\Omega_X^2 + 2w^2}{2\tau\Omega_X} - w^2 \right\} - \frac{w \exp \left( -w^2 \left( \tau - \frac{2}{\Omega_X} \right) \right)}{2\tau^2\Omega_X} \right], w < 0. \quad (30) \\ & \frac{4e^{-w^2/\Omega_X}}{\Omega_X \Omega_Y} \left[ \frac{\sqrt{\pi} \operatorname{erfc} \left( \frac{w}{\sqrt{\tau}\Omega_X} \right) \exp \left( \frac{w^2}{\tau\Omega_X^2} \right)}{2\tau^{\frac{3}{2}}\Omega_X} \times \right. \\ & \left. \left\{ \frac{\tau\Omega_X^2 + 2w^2}{2\tau\Omega_X} - w^2 \right\} + \frac{w}{2\tau} \left( 1 - \frac{1}{\tau\Omega_X} \right) \right], w \geq 0. \end{aligned}$$

In (30),  $\tau = \frac{\Omega_X + \Omega_Y}{\Omega_X \Omega_Y}$ ,  $\Omega_X = \frac{\epsilon_1}{N_0} E[|h_1|^2]$ ,  $\Omega_Y = \frac{2\epsilon_2}{N_0} E[|h_2|^2]$  and  $\operatorname{erfc}(x) = 1 - \operatorname{erf}(x)$ .

The average bit error probability of NU for UL-NOMA becomes

$$\begin{aligned} \overline{P_1(e)} = & \frac{1}{2} \left[ \int_0^\infty Q(\sqrt{\gamma_H}) f_{\gamma_H}(\gamma_H) d\gamma_H \right. \\ & \left. + \frac{1}{2} \left\{ \int_0^\infty Q(z) f_Z(z) dz + \int_0^\infty Q(w) f_W(w) dw \right\} \right], \end{aligned} \quad (31)$$

where

$$\gamma_H = \frac{\epsilon_1 \times |h_1|^2}{N_0}, \quad \overline{\gamma_H} = \frac{\epsilon_1}{N_0} E[|h_1|^2] \quad (32)$$

are defined as in (6).

The first term in (31) can be expressed in a closed form. Then the error probability of NU for UL-NOMA turns out to be

$$\begin{aligned} \overline{P_1(e)} = & \frac{1}{4} \left[ \left( 1 - \sqrt{\frac{\overline{\gamma}_H}{2 + \overline{\gamma}_H}} \right) \right. \\ & \left. + \int_0^\infty Q(z) f_Z(z) dz + \int_0^\infty Q(w) f_W(w) dw \right]. \end{aligned} \quad (33)$$

To detect FU symbols, BS subtracts regenerated NU symbols after detecting NU symbols. In this case, two different cases may occur, which are NU symbols are detected correctly or erroneously. To analyse FU error performance for UL-NOMA, these two different cases should be handled as in the NU error performance derivation for DL-NOMA. However, it should be taken into consideration that only the decision for the first bit of  $x_1$  symbols effects the FU error performance. The decision for second bit of  $x_1$  symbol has no role on the decision of FU symbols. The signal spaces for the scenarios FU symbols are detected correctly and erroneously are given in Fig. 3b and c, respectively. Neither the noise in the quadrature phase nor the component occurred after subtracting NU symbols from received signal has a role on deciding FU symbols. Therefore, these values are not presented in Fig. 3b and c.

We first consider that NU symbols are detected correctly. In this case, the probability of the correct decoding for the first bit of the NU symbol will be equal to the priori probabilities of the symbols given in Fig. 3b. The error probabilities of each symbol given in Fig. 3b can be easily obtained by considering the decision boundary given in Fig. 3b as in (4). Hence, the error probability of the symbols for FU under the assumption that the first bit of the NU symbols detected correctly is defined as

$$\begin{aligned} P_2(e|\text{correct}_{\text{NU}}) = & \frac{1}{2} \left[ P_r \left( n_1 \leq \sqrt{\frac{\epsilon_1}{2}} h_1 + \sqrt{\epsilon_2} h_2 \right) \right. \\ & \times P_r \left( n_1 \geq \sqrt{\epsilon_2} h_2 \middle| n_1 \leq \sqrt{\frac{\epsilon_1}{2}} h_1 + \sqrt{\epsilon_2} h_2 \right) \\ & + P_r \left( n_1 \leq \sqrt{\frac{\epsilon_1}{2}} h_1 - \sqrt{\epsilon_2} h_2 \right) \\ & \left. \times P_r \left( n_1 \leq -\sqrt{\epsilon_2} h_2 \middle| n_1 \leq \sqrt{\frac{\epsilon_1}{2}} h_1 - \sqrt{\epsilon_2} h_2 \right) \right]. \end{aligned} \quad (34)$$

The conditional expressions are the error probabilities of the  $x_2$  symbols given in Fig. 3b. The conditions define that the events of the first bits of the given NU symbols are detected correctly. By using (15), it can be defined as

$$\begin{aligned} P_2(e|\text{correct}_{\text{NU}}) = & \frac{1}{2} \left[ P_r \left( \sqrt{\epsilon_2} h_2 \leq n_1 \leq \sqrt{\frac{\epsilon_1}{2}} h_1 + \sqrt{\epsilon_2} h_2 \right) \right. \\ & \left. + P_r \left( n_1 \leq -\sqrt{\epsilon_2} h_2 \right) \right]. \end{aligned} \quad (35)$$

With the aid of PDF definition given in (29), the error probability of FU under the condition that NU symbols are detected correctly at BS, is given as

$$P_2(e|\text{correct}_{\text{NU}}) = Q(\sqrt{\gamma_j}) - \frac{Q(z)}{2}, \quad (36)$$

where  $\gamma_J$  and  $\bar{\gamma}_J$  are defined similar to (6) as

$$\gamma_J = \frac{2\epsilon_2 \times |h_2|^2}{N_0}, \quad \bar{\gamma}_J = \frac{2\epsilon_2}{N_0} E[|h_2|^2]. \quad (37)$$

On the other hand, the error probability of FU under the condition that NU symbols are detected erroneously, is given as

$$\begin{aligned} P_2(e|\text{error}_{\text{NU}}) &= \frac{1}{2} \left[ P_r \left( n_1 \geq \sqrt{\frac{\epsilon_1}{2}} h_1 + \sqrt{\epsilon_2} h_2 \right) \right. \\ &\quad \times P_r \left( n_1 \geq 2\sqrt{\frac{\epsilon_1}{2}} h_1 + \sqrt{\epsilon_2} h_2 \middle| n_1 \geq \sqrt{\frac{\epsilon_1}{2}} h_1 + \sqrt{\epsilon_2} h_2 \right) \\ &\quad + P_r \left( n_1 \geq \sqrt{\frac{\epsilon_1}{2}} h_1 - \sqrt{\epsilon_2} h_2 \right) \\ &\quad \left. \times P_r \left( n_1 \leq 2\sqrt{\frac{\epsilon_1}{2}} h_1 - \sqrt{\epsilon_2} h_2 \middle| n_1 \geq \sqrt{\frac{\epsilon_1}{2}} h_1 - \sqrt{\epsilon_2} h_2 \right) \right]. \end{aligned} \quad (38)$$

The expression given in (38) is obtained as in (34). The prior probabilities have been replaced with the error probabilities for the first bits of the symbols for NU. Then, the error probabilities of the FU symbols ( $x_2$ ) given in Fig. 3c are obtained by considering the decision boundary given in Fig. 3c as in (4). The conditions define that the events first bits of the given NU symbols are detected erroneously.

By using (15), the error probability for FU under the assumption of the first bit of the NU symbols detected erroneously becomes

$$P_2(e|\text{error}_{\text{NU}}) = \frac{1}{2} [Q(w) + Q(\nu) - Q(\kappa)]. \quad (39)$$

where  $\nu$  is the sum of two Rayleigh distributed variables and the PDF of  $\nu$  is likely PDF of  $z$  given in (31), where  $a_1 = \sqrt{2\epsilon_1/N_0 E[|h_1|^2]}$  and  $a_2 = \sqrt{\epsilon_2/N_0 E[|h_2|^2]}$ . Also,  $\kappa$  is the difference of two Rayleigh distributed variables and the PDF of  $\kappa$  is likely PDF of  $w$  given in (30), where  $\Omega_X = 4\epsilon_1/N_0 E[|h_1|^2]$  and  $\Omega_Y = 2\epsilon_2/N_0 E[|h_2|^2]$ .

Then, total error probability of FU for UL-NOMA is derived as the sum of two different cases which are NU symbols detected correctly or erroneously. Consequently, the sum of (36) and (39) can be written as

$$P_2(e) = Q(\sqrt{\gamma_J}) + \frac{1}{2} [Q(w) - Q(z) + Q(\nu) - Q(\kappa)]. \quad (40)$$

Finally, the average BER of FU for UL-NOMA is derived as

$$\begin{aligned} \overline{P_2(e)} &= \int_0^\infty Q(\sqrt{\gamma_J}) f_{\gamma_J}(\gamma_J) d\gamma_J + \frac{1}{2} \left[ \int_0^\infty Q(w) f_W(w) dw \right. \\ &\quad - \int_0^\infty Q(z) f_Z(z) dz + \int_0^\infty Q(\nu) f_\nu(\nu) d\nu \\ &\quad \left. - \int_0^\infty Q(\kappa) f_\kappa(\kappa) d\kappa \right]. \end{aligned} \quad (41)$$

At this point, the above expression can be defined in the one-degree integral form as (see (42)).

To the best of our knowledge, it is not possible to derive closed-form expressions for the integrals in (33) and (42). Nevertheless, these single-integral form derivations can be easily evaluated numerically by mathematical programs such as MATLAB,

MATHEMATICA and MAPLE. Besides, closed-form expressions are derived for approximate expressions instead of exact expressions for uplink. The derivation of approximate expressions above will be given in the next sub-section.

### 3.3 Approximate BER expressions for UL-NOMA

Considering the values of Gaussian  $Q$  function, it can be easily seen that

$$Q(a-b) \gg Q(a+b) \quad \text{when } a, b \text{ positive.} \quad (43)$$

By using (43), the second term in (33) can be neglected and the error probability of NU for UL-NOMA can be approximated as

$$\overline{P_1(e)} \simeq \frac{1}{4} \left[ \left( 1 - \sqrt{\frac{\gamma_H}{1 + \gamma_H}} \right) + \int_0^\infty Q(w) f_W(w) dw \right]. \quad (44)$$

The second term in (44) is given by

$$\begin{aligned} \overline{P} &= \int_0^\infty Q(w) f_W(w) dw \\ &= \int_0^\infty \int_0^\infty Q \left( \frac{\sqrt{\epsilon_1/2} h_1 - \sqrt{\epsilon_2} h_2}{\sqrt{N_0}} \right) f_{h_1}(h_1) dh_1 f_{h_2}(h_2) dh_2. \end{aligned} \quad (45)$$

Without loss of generality, we assume that first bit of NU is  $i_{1,1} = 0$ . In this case, by considering signal space given in Fig. 3b, the error will occur when the in-phase component of received signal is lower than 0 ( $y_1 < 0$ ). It is clear that, the error probability of the first bit of NU mostly effected by the difference of symbol energies due to the fading rather than the noise. As  $\sqrt{\epsilon_1} h_1 = \sqrt{\epsilon_2} h_2$ , an error will occur with high probability, even if the noise is very low and  $\epsilon_1$  and  $\epsilon_2$  are very high. Considering this, the first bit of NU is detected erroneously if  $\sqrt{\epsilon_1/2} h_1 - \sqrt{\epsilon_2} h_2 < 0$ . Hence, the probability given in (45) can be redefined as

$$\overline{P} \simeq \int_0^\infty \int_0^\mu f_\rho(\rho) d\rho f_\mu(\mu) d\mu. \quad (46)$$

where  $\rho = \sqrt{\epsilon_1/2} h_1$  and  $\mu = \sqrt{\epsilon_2} h_2$ . Due to the fact that  $h_1$  and  $h_2$  are Rayleigh distributed,  $\rho$  and  $\mu$  are also Rayleigh distributed with different variances. Then, by substituting Rayleigh PDFs into (46) gives

$$\overline{P} \simeq \int_0^\infty \int_0^\mu \frac{\mu}{\Omega_\mu} e^{-(\mu^2/\Omega_\mu)} \frac{\rho}{\Omega_\rho} e^{-(\rho^2/\Omega_\rho)} d\mu d\rho. \quad (47)$$

After some algebraic manipulations, it can be determined as

$$\overline{P} \simeq \frac{\Omega_\mu}{\Omega_\mu + \Omega_\rho}, \quad (48)$$

where

$$\Omega_\rho = \epsilon_1/2 E[|h_1|^2], \quad \Omega_\mu = \epsilon_2 E[|h_2|^2]. \quad (49)$$

Finally, by substituting (48) into (44), the average BER expression of NU for UL-NOMA becomes

$$\overline{P_1(e)} \simeq \frac{1}{4} \left[ \left( 1 - \sqrt{\frac{\gamma_H}{2 + \gamma_H}} \right) + \frac{\Omega_\mu}{\Omega_\mu + \Omega_\rho} \right]. \quad (50)$$

---


$$\begin{aligned} \overline{P_2(e)} &= \frac{1}{2} \left[ \left( 1 - \sqrt{\frac{\gamma_J}{2 + \gamma_J}} \right) + \int_0^\infty Q(w) f_W(w) dw \right. \\ &\quad \left. - \int_0^\infty Q(z) f_Z(z) dz + \int_0^\infty Q(\nu) f_\nu(\nu) d\nu - \int_0^\infty Q(\kappa) f_\kappa(\kappa) d\kappa \right]. \end{aligned} \quad (42)$$

To derive approximate BER of FU for UL-NOMA, exact average BER expression given in (41) can be approximated as in (51) when  $Q(z)$  and  $Q(v)$  are neglected, considering it has  $Q(w)$  and  $Q(\kappa)$  terms by using (43)

$$\overline{P_2(e)} \simeq \frac{1}{2} \left[ \left( 1 - \sqrt{\frac{\gamma_J}{2 + \gamma_J}} \right) + \int_0^\infty Q(w) f_W(w) dw - \int_0^\infty Q(\kappa) f_\kappa(\kappa) dk \right]. \quad (51)$$

After that, taking the steps through (46)–(48) for the third term in (51)

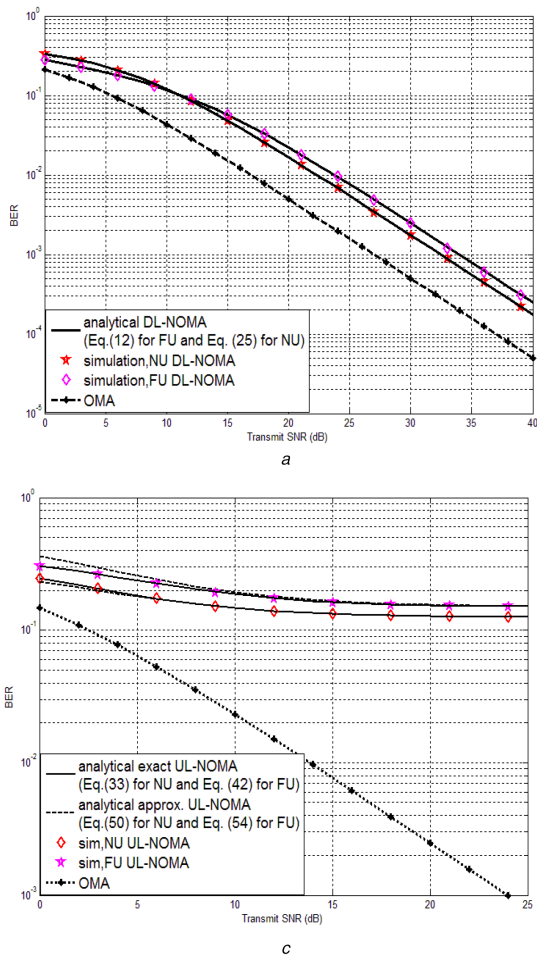
$$\int_0^\infty Q(\kappa) f_\kappa(\kappa) dk \simeq \frac{\Omega_\mu}{\Omega_\eta + \Omega_\mu} \quad (52)$$

is obtained. In (52), the variance is given by

$$\Omega_\eta = 2\epsilon_1 E[|h_1|^2]. \quad (53)$$

By substituting (48) and (52) into (51), the approximate expression for the BER of FU is derived as

$$\overline{P_2(e)} \simeq \frac{1}{2} \left[ \left( 1 - \sqrt{\frac{\gamma_J}{2 + \gamma_J}} \right) + \frac{\Omega_\mu}{\Omega_\mu + \Omega_\rho} - \frac{\Omega_\mu}{\Omega_\eta + \Omega_\mu} \right]. \quad (54)$$



#### 4 Numerical results

In this section, we numerically calculate the probability of error performances by using the above derived equations, then validate the results by using simulations. The exact expressions derived in the previous section match perfect with simulation results for both DL-NOMA and UL-NOMA. Furthermore, the approximate derivations for UL-NOMA match quite well with the simulations.

In Fig. 4, a comparison of OMA and NOMA schemes is given for both downlink and uplink. In Fig. 4a, the BER comparison of OMA and DL-NOMA over Rayleigh fading channels is presented by using the expressions in (12) for FU and (25) for NU, and by changing the transmit SNR of the BS. In the calculations, the average variances for NU ( $\Omega_1 = E[|h_1|^2]$ ) and FU ( $\Omega_2 = E[|h_2|^2]$ ) are considered as 0 and  $-3$  dB, respectively. In DL-NOMA, the power allocation coefficient is chosen as  $\alpha = 0.4$ . It is assumed that OMA users are implemented by TDMA and each user covers half of one time slot. BER performances of OMA users are better than those of the NOMA scheme, because OMA users do not encounter any inter-user interferences (IUIs). However, this performance decay of NOMA should be evaluated with the capacity/throughput and outage performance gains of NOMA given in [34, 35]. To demonstrate one of these NOMA gains, the ergodic sum rate comparison of DL-NOMA and OMA is given in Fig. 4b. The rates of users for DL-NOMA are obtained by  $R_i = \log_2(\text{SINR}_i)$ ,  $i = 1, 2$ , where  $\text{SINR}_1 = \alpha P_s |h_1|^2 / ((1 - \alpha) P_s |h_1|^2 + N_0)$  and  $\text{SINR}_2 = (1 - \alpha) P_s |h_2|^2 / (\alpha P_s |h_2|^2 + N_0)$  [34, 35]. For OMA users, rates are given by  $R_i = 1/2 \log_2(\text{SNR}_i)$ ,  $i = 1, 2$ , where  $\text{SNR}_i$  is the signal-to-noise

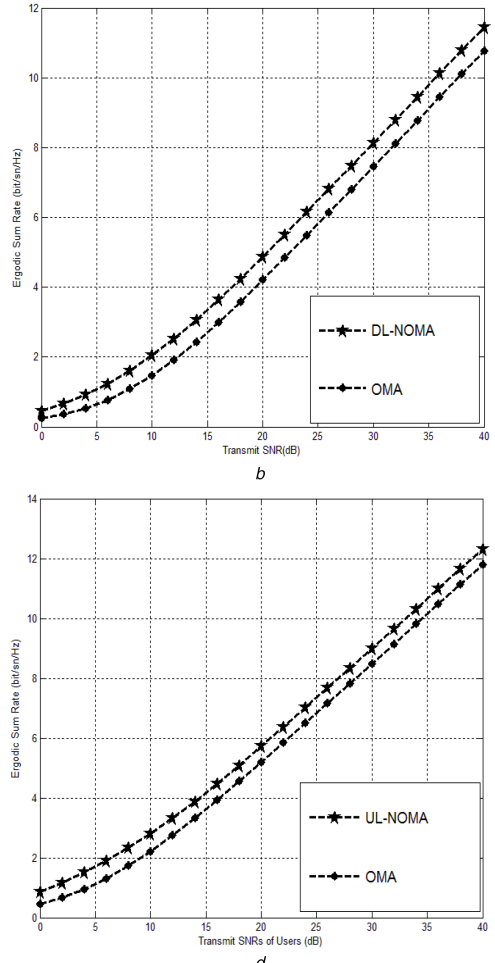
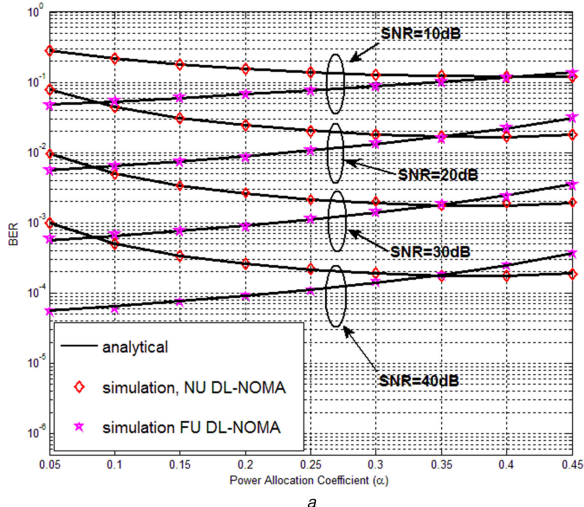
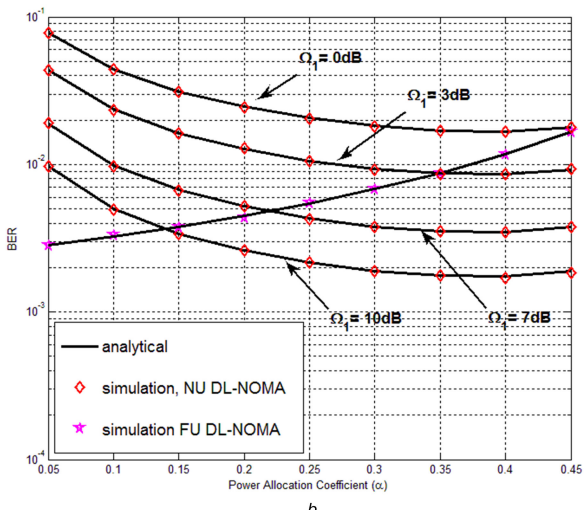


**Fig. 4** Comparison of OMA and NOMA schemes for downlink and uplink

- (a) BER comparison of NOMA and OMA for downlink,
- (b) Ergodic sumrate comparison of NOMA and OMA for downlink,
- (c) BER comparison of NOMA and OMA for uplink,
- (d) Ergodic sumrate comparison of NOMA and OMA for uplink



a



b

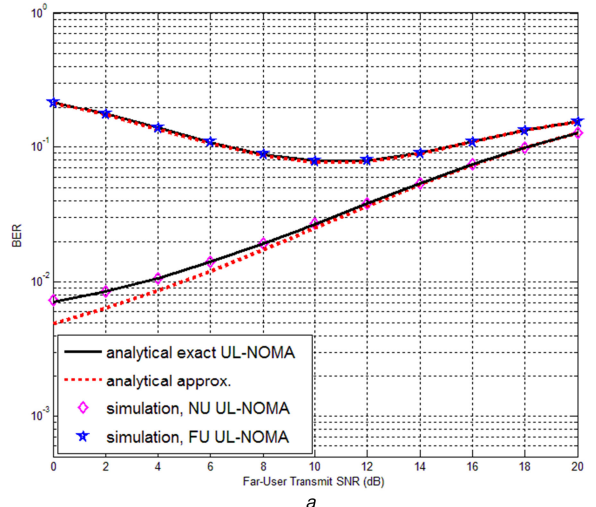
**Fig. 5** Effect of power allocation coefficient on the BER performances for DL-NOMA

(a)  $\Omega_1 = E[|h_1|^2] = 0 \text{ dB}$ ;  $\Omega_2 = E[|h_2|^2] = -3 \text{ dB}$ ,

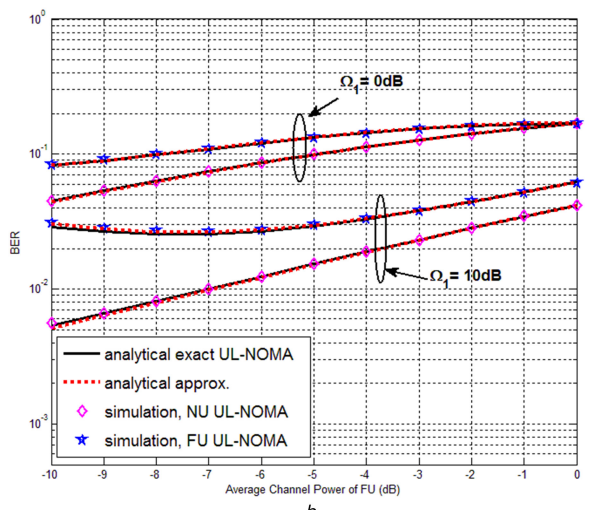
(b)  $\Omega_2 = E[|h_2|^2] = 0 \text{ dB}$ ;  $\text{SNR} = 20 \text{ dB}$

ratio (no interference) of  $i$  user. The coefficient  $1/2$  exists for OMA users because each user transmits only half of time. In Fig. 4c, the BER comparison of OMA and UL-NOMA is given with the change of transmit SNR in the scenario that both users have the same transmit SNR ( $P_1 = P_2$ ). The analytical results show the numerically calculations by using (33) and (50) for NU and by using (42) and (54) for FU for the exact and approximate results, respectively. For Rayleigh fading channels,  $\Omega_1 = E[|h_1|^2] = 0 \text{ dB}$  and  $\Omega_2 = E[|h_2|^2] = -3 \text{ dB}$ . It can be seen that, increasing transmit powers of both users does not ensure a gain in BER performance for UL-NOMA because it also means an increase in IUI. OMA users have better BER performance compared to UL-NOMA as in DL-NOMA. However, UL-NOMA also ensures better outage and capacity performance than OMA. For a fair evaluation, the ergodic sum rate comparison for OMA and UL-NOMA is given in Fig. 4d. The rates of UL-NOMA users are obtained as DL-NOMA where  $\text{SINR}_1 = \alpha P_1 |h_1|^2 / (P_2 |h_2|^2 + N_0)$  and  $\text{SINR}_2 = P_2 |h_2|^2 / (P_1 |h_1|^2 + N_0)$ . For OMA users, the rates are given as explained above.

To uncover the role of power allocation coefficient on the BER performances of users for DL-NOMA, simulation results are given in Fig. 5. In Fig. 5a, BER performances of users are given with the change of  $\alpha$  for the different values of transmit SNR, i.e. SNR = 10, 20, 30 and 40 dB. In this scenario, average channel coefficient powers are modelled as  $\Omega_1 = E[|h_1|^2] = 0 \text{ dB}$  for NU and  $\Omega_2 = E[|h_2|^2] = -3 \text{ dB}$  for FU. It is seen that, increase of  $\alpha$  does not always ensure a gain in BER performance of NU, although it always causes a decay in FU's. Since, decreasing transferred power



a



b

**Fig. 6** BER performances of users for UL-NOMA

(a)  $\Omega_1 = E[|h_1|^2] = 0 \text{ dB}$ ;  $\Omega_2 = E[|h_2|^2] = -3 \text{ dB}$ ,  $\text{SNR}_1 = 20 \text{ dB}$ ,

(b)  $\text{SNR}_1 = \text{SNR}_2 = 20 \text{ dB}$

to FU symbols causes FU symbols to be detected erroneously by SIC implemented at NU. This SIC error from FU symbols will have dominant effect on NU performance when  $\alpha$  is increased too much. To examine the effect of  $\alpha$  in detail, in Fig. 5b, BER performances of users for DL-NOMA are presented with transmit SNR = 20 dB with respect to  $\alpha$  on the scenarios which have different channel quality of NU where  $\Omega_2 = E[|h_2|^2] = 0 \text{ dB}$  and  $\Omega_1 = E[|h_1|^2] = 0, 3, 7$  and  $10 \text{ dB}$ . It is again seen that, increasing of  $\alpha$  causes a decay in BER performance of NU because of the SIC error from FU symbols. In order to obtain an optimum power allocation coefficient for DL-NOMA, these BER constrains should be considered. It is clear that, this optimum threshold value should be adapted according to transmit SNR and channel qualities of users.

Fig. 6 presents the BER performances of users for UL-NOMA. In Fig. 6a, BER performances are given with respect to the FU transmit SNR. It is assumed that, NU has fixed 20 dB transmit SNR and average channel coefficient powers are modelled as  $\Omega_1 = E[|h_1|^2] = 0 \text{ dB}$  for NU and  $\Omega_2 = E[|h_2|^2] = -3 \text{ dB}$ . It is seen that BER performance of NU given in (33) and (50) for the exact and approximate results, respectively, decrease when the transmit power of FU increases. This is because of the increased IUI NU encounter. Due to the SIC error from NU symbols to FU, the increment of the transmit power also does not always ensure a performance gain for FU. The approximate expressions for the UL-NOMA are obtained by considering the fact given in (43). On the other hand, when the value of the parameter  $a$  is much higher than the value of  $b$  (i.e.  $a \gg b$ ), the values of the  $Q$  functions in (43) get

closer. Hence, the second term of the error probability expression in (27) becomes dominant on the error probability of FU when the SNR difference of FU and NU is large. Consequently, the small gap between the numerical values of the derived exact and approximate expression occurs when the channel conditions affected by SNR and fading of FU and NU differ substantially. Nevertheless, this effect does not appear on the values obtained by the derived expressions for the FU. As the omitted third and fourth terms in (42) have opposite signs (positive and negative), they compensate each other's effect on the error probability of NU.

In order to show the effect of channel conditions on the BER performances for UL-NOMA, performances are given with respect to the channel quality of FU defined by  $\Omega_2$  in Fig. 6b. For two different  $\Omega_2$  values, performances are investigated when the transmit SNRs of users are equal. It is seen that, increasing channel quality of FU causes a performance decay for both users. Also, it is clear that both users have better error performance when the NU has better channel quality. It can be explained as,

- Better channel quality of NU brings an opportunity to suppress IUI for NU
- Better channel quality of NU reduces the SIC error from NU to FU when SIC is implemented.

## 5 Conclusions

In this paper, for the first time in the literature, exact BER expressions are derived for both DL-NOMA and UL-NOMA schemes in the presence of SIC errors over Rayleigh fading channels. The exact BER expressions is given in closed-form for DL-NOMA, but it is given only in one-degree integral form for uplink. Nevertheless, we also provide a closed-form expression of the approximate BER for UL-NOMA. Furthermore, the PDF of the difference of two i.n.i.d Rayleigh distributions is derived. All the derived expressions are verified with the computer simulations.

Based on the numerical results obtained via the derived equations, the effect of power allocation coefficient on DL-NOMA users' performances is investigated. The results show that, the  $\alpha$  coefficient changes performances of users substantially. It is shown that power allocation coefficient should be adapted according to channel conditions between BS and user in addition to transmitted SNR.

The difference of channel qualities and power of users have dominant effect on BER performances of users for UL-NOMA, whereas the increment of transmit powers for both users does not ensure a performance gain. Based on the numerical results, UL-NOMA is efficient when the users' distance from the BS are different.

The analytical BER expressions derived in this paper could be easily extended for higher order modulation levels ( $M$ -ary modulation). For  $M$ -ary modulation, the priori probabilities and energy levels according to considered modulation level should be modified in the derived equations in Section 3. In addition, the derived expressions can be used for the BER analysis of the more complex NOMA systems. In particular, the error probability for FU calculated at the NU due to the SIC error represents the probability of the error propagation phenomena may occur in cooperative-NOMA systems. Additionally, the derived expressions represent the error probability of the users in the second phase of the relay-aided NOMA systems. As the channel coefficients are in the matrix form in the MIMO-NOMA, the extension of the derived BER expressions to MIMO-NOMA requires more effort. Consequently, the closed-form BER analysis of conventional NOMA systems with the  $M$ -ary modulations and the NOMA involved systems such as MIMO-NOMA, cooperative-NOMA and relay-aided NOMA systems are beyond the scope of this paper and considered as future works.

## 6 Acknowledgments

This project is supported by The Scientific and Technological Research Council of Turkey (TÜBİTAK) under the 2211-E PhD Scholarship Program.

## 7 References

- [1] Boccardi, F., Marzetta, T.L., Labs, B.: 'Five disruptive technology directions for 5G', *IEEE Commun. Mag.*, 2014, (February), pp. 74–80
- [2] Andrews, J.G., Buzzi, S., Choi, W., et al.: 'What will 5G be?', *IEEE J. Sel. Areas Commun.*, 2014, **32**, (6), pp. 1065–1082
- [3] Dai, L., Wang, B., Yuan, Y., et al.: 'Non-orthogonal multiple access for 5G: solutions, challenges, opportunities, and future research trends', *IEEE Commun. Mag.*, 2015, **53**, (9), pp. 74–81
- [4] Higuchi, K., Benjebbour, A.: 'Non-orthogonal multiple access (NOMA) with successive interference cancellation for future radio access', *IEICE Trans. Commun.*, 2015, **E98.B**, (3), pp. 403–414
- [5] Shin, W., Vaezi, M., Lee, B., et al.: 'Non-orthogonal multiple access in multi-cell networks: theory, performance, and practical challenges', *IEEE Commun. Mag.*, 2017, (October), pp. 176–183
- [6] Saito, Y., Kishiyama, Y., Benjebbour, A., et al.: 'Non-orthogonal multiple access (NOMA) for cellular future radio access'. IEEE Vehicular Technology Conf. (VTC Spring), Dresden, 2013, pp. 1–5
- [7] Timotheou, S., Krikidis, I.: 'Fairness for non-orthogonal multiple access in 5G systems', *IEEE Signal Process. Lett.*, 2015, **22**, (10), pp. 1647–1651
- [8] Cui, J., Liu, Y., Ding, Z., et al.: 'Optimal user scheduling and power allocation for millimeter wave NOMA systems', *IEEE Trans. Wireless Commun.*, 2018, **17**, (3), pp. 1502–1517
- [9] Ding, Z., Schober, R., Poor, H.V.: 'A general MIMO framework for NOMA downlink and uplink transmission based on signal alignment', *IEEE Trans. Wirel. Commun.*, 2016, **15**, (6), pp. 4438–4448
- [10] Cui, J., Ding, Z., Fan, P.: 'A novel power allocation scheme under outage constraints in NOMA systems', *IEEE Signal Process. Lett.*, 2016, **23**, (9), pp. 1226
- [11] Choi, J.: 'On the power allocation for MIMO-NOMA systems with layered transmissions', *IEEE Trans. Wirel. Commun.*, 2016, **15**, (5), pp. 3226–3237
- [12] Oviedo, J.A., Sadjadpour, H.R.: 'A fair power allocation approach to NOMA in multiuser SISO systems', *IEEE Trans. Veh. Technol.*, 2017, **66**, (9), pp. 7974–7985
- [13] Guo, J., Wang, X., Yang, J., et al.: 'User pairing and power allocation for downlink non-orthogonal multiple access'. 2016 IEEE Globecom Workshops (GC Wkshps), Washington, DC, 2016, pp. 1–6
- [14] Zhang, H., Zhang, D.K., Meng, W.X., et al.: 'User pairing algorithm with SIC in non-orthogonal multiple access system'. 2016 IEEE Int. Conf. Commun. (ICC 2016), Kuala Lumpur, 2016, pp. 1–6
- [15] Ali, M.S., Tabassum, H., Hossain, E.: 'Dynamic user clustering and power allocation for uplink and downlink non-orthogonal multiple access (NOMA) systems', *IEEE Access*, 2016, **4**, pp. 6325–6343
- [16] Sun, Q., Hanl, S., Chin-Lin, I., et al.: 'On the ergodic capacity of MIMO NOMA systems', *IEEE Wirel. Commun. Lett.*, 2015, **4**, (4), pp. 405–408
- [17] Benjebbour, A., Li, A., Kishiyama, Y., et al.: 'System-level performance of downlink NOMA combined with SU-MIMO for future LTE enhancements'. 2014 IEEE Globecom Workshops (GC Wkshps), Austin, TX, 2014, pp. 706–710
- [18] Haci, H., Zhu, H., Wang, J.: 'Performance of non-orthogonal multiple access with a novel asynchronous interference cancellation technique', *IEEE Trans. Commun.*, 2017, **65**, (3), pp. 1319–1335
- [19] Wang, X., Labreau, F., Mei, L.: 'Closed-form BER expressions of QPSK constellation for uplink non-orthogonal multiple access', *IEEE Commun. Lett.*, 2017, **21**, (10), pp. 2242–2245
- [20] Al-Imari, M., Xiao, P., Imran, M.A., et al.: 'Uplink non-orthogonal multiple access for 5G wireless networks'. 2014 11th Int. Symp. Wirel. Commun. Syst. (ISWCS), Barcelona, 2014, pp. 781–785
- [21] Usman, M.R., Khan, A., Usman, M.A., et al.: 'On the performance of perfect and imperfect SIC in downlink non orthogonal multiple access (NOMA)'. 2016 Int. Conf. Smart Green Technol. Electr. Inf. Syst. (ICSGTEIS), Bali, 2016, 102–106
- [22] Sun, Q., Han, S., Chin-Lin, I., et al.: 'On the ergodic capacity of MIMO NOMA systems', *IEEE Wirel. Commun. Lett.*, 2015, **4**, (4), pp. 405–408
- [23] Ding, Z., Schober, R., Poor, H.V.: 'A general MIMO framework for NOMA downlink and uplink transmission based on signal alignment', *IEEE Trans. Wirel. Commun.*, 2016, **15**, (6), pp. 4438–4454
- [24] Ding, Z., Peng, M., Poor, H.V.: 'Cooperative non-orthogonal multiple access in 5G systems', *IEEE Commun. Lett.*, 2015, **19**, (8), pp. 1462–1465
- [25] Ding, Z., Dai, H., Poor, H.V.: 'Relay selection for cooperative NOMA', *IEEE Trans. Veh. Technol.*, 2016, **5**, (4), pp. 416–419
- [26] Ge, J., Men, J.: 'Performance analysis of non-orthogonal multiple access in downlink cooperative network', *IET Commun.*, 2015, **9**, (18), pp. 2267–2273
- [27] Lee, S., Vien, Q., Duong, T.Q.: 'Non-orthogonal multiple access schemes with partial relay selection', *IET Commun.*, 2017, **11**, (6), pp. 846–854
- [28] Zhang, Z., Ma, Z., Xiao, M., et al.: 'Full-duplex device-to-device-aided cooperative nonorthogonal multiple access', *IEEE Trans. Veh. Technol.*, 2017, **66**, (5), pp. 4467–4471
- [29] Zhong, C., Zhang, Z.: 'Non-orthogonal multiple access with cooperative full-duplex relaying', *IEEE Commun. Lett.*, 2016, **20**, (12), pp. 2478–2481
- [30] Craig, J.W.: 'A new, simple and exact result for calculating the probability of error for two-dimensional signal constellations'. MILCOM 91 - Conf. Rec., McLean, VA, USA, 1991, **2**, pp. 571–575
- [31] Gradshteyn, I.S., Ryzhik, I.M.: 'Table of integrals, series, and products' (Academic Press, New York, 1994, 5th edn.)
- [32] Simon, M.K., Alouini, M.-S.: 'Digital communication over fading channels' (John Wiley & Sons, Inc., New York, 2004)
- [33] Archer, C.O.: 'Some Properties of Rayleigh Distributed Random Variables and of Their Sums and Products', 1967

- [34] Ding, Z., Yang, Z., Fan, P., et al.: ‘On the performance of non-orthogonal multiple access in 5G systems with randomly deployed users’, *IEEE Signal Process. Lett.*, 2014, **21**, (12), pp. 1501–1505
- [35] Saito, Y., Benjebbour, A., Kishiyama, Y., et al.: ‘System-level performance evaluation of downlink non-orthogonal multiple access (NOMA)’. IEEE Int. Symp. Pers. Indoor Mob. Radio Commun. PIMRC, London, 2013, pp. 611–615
- [36] Woods, F.S.: ‘*Differentiation of a definite integral advanced calculus: A course arranged with special reference to the needs of students of applied mathematics*’ (Ginn, Boston, MA, 1926)

## 8 Appendix

### 8.1 Proof of (30)

Let we define a random variable (RV)  $W = X - Y$ , where  $X$  and  $Y$  are RVs. The cumulative distribution function of  $W$  is given as

$$F_W(w) = P_r(W \leq w) = P_r(X - Y \leq w) = P_r(X \leq w + Y), \quad (55)$$

$$F_W(w) = \int_{-\infty}^{\infty} \int_{-\infty}^{w+y} f_{XY}(x, y) dx dy. \quad (56)$$

PDF of  $W$  is given by

$$f_W(w) = \frac{dF_W(w)}{dw} = \int_{-\infty}^{\infty} \frac{d}{dw} \left( \int_{-\infty}^{w+y} f_{XY}(x, y) dx \right) dy. \quad (57)$$

By using the Leibniz integral rule [36], it can be expressed as

$$f_W(w) = \int_{-\infty}^{\infty} f_{XY}(w + y, y) dy. \quad (58)$$

If  $X$  and  $Y$  are independent Rayleigh random variables, i.e.  $x \geq 0$  and  $y \geq 0$

$$f_W(w) = \begin{cases} \int_{-w}^{\infty} f_X(w + y) f_Y(y) dy, & w < 0, \\ \int_0^{\infty} f_X(w + y) f_Y(y) dy, & w \geq 0. \end{cases} \quad (59)$$

In case  $X$  and  $Y$  are Rayleigh distributions, the PDF of  $X$  and  $Y$  is given as

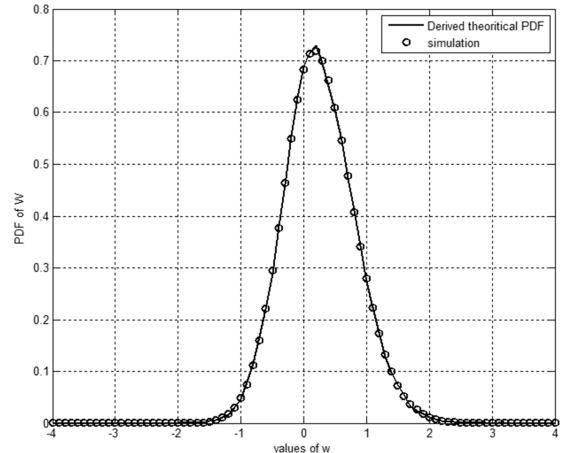


**Fig. 7** Derived PDF of the difference of two i.n.i.d Rayleigh distributions

$$\begin{aligned} f_X(x) &= \frac{2x}{\Omega_X} \exp\left(-\frac{x^2}{\Omega_X}\right), \quad x \geq 0, \\ f_Y(y) &= \frac{2y}{\Omega_Y} \exp\left(-\frac{y^2}{\Omega_Y}\right), \quad y \geq 0. \end{aligned} \quad (60)$$

where  $\Omega_X = E[|X|^2]$  and  $\Omega_Y = E[|Y|^2]$ .

Substituting (60) into (59)

$$f_W(w) = \begin{cases} \int_{-w}^{\infty} \frac{2(w+y)}{\Omega_X} \exp\left(-\frac{(w+y)^2}{\Omega_X}\right) \frac{2y}{\Omega_Y} \exp\left(-\frac{y^2}{\Omega_Y}\right) dy, & w < 0, \\ \int_0^{\infty} \frac{2(w+y)}{\Omega_X} \exp\left(-\frac{(w+y)^2}{\Omega_X}\right) \frac{2y}{\Omega_Y} \exp\left(-\frac{y^2}{\Omega_Y}\right) dy, & w \geq 0. \end{cases} \quad (61)$$

After some algebraic manipulations, the PDF of  $W$  is derived as in (30). To verify the derived PDF, simulation result is given in Fig. 7 for  $\Omega_X = 0$  dB and  $\Omega_Y = -3$  dB.